J|A|C|S ARTICLES

Published on Web 01/07/2010

Ultrafast Optical Excitations In Supramolecular Metallacycles with Charge Transfer Properties

Daniel C. Flynn,[†,‡] Guda Ramakrishna,[§] Hai-Bo Yang,[||] Brian H. Northrop,[⊥] Peter J. Stang,*[,⊥] and Theodore Goodson III*[,†,‡]

Department of Chemistry and Department of Macromolecular Science and Engineering, University of Michigan, Ann Arbor, Michigan 48109, Department of Chemistry, Western Michigan University, Kalamazoo Michigan 49008, Department of Chemistry, University of Utah, Utah, and Shanghai Key Laboratory of Green Chemistry and Chemical Processes, Department of Chemistry, East China Normal University, 3663 North Zhongshan Road, Shanghai 200062, China

Received September 28, 2009; E-mail: tgoodson@umich.edu; Stang@chem.utah.edu

Abstract: New organometallic materials such as two-dimensional metallacycles and three-dimensional metallacages are important for the development of novel optical, electronic, and energy related applications. In this article, the ultrafast dynamics of two different platinum-containing metallacycles have been investigated by femtosecond fluorescence upconversion and transient absorption. These measurements were carried out in an effort to probe the charge transfer dynamics and the rate of intersystem crossing in metallacycles of different geometries and dimensions. The processes of ultrafast intersystem crossing and charge transfer vary between the two different classes of metallacyclic systems studied. For rectangular anthracene-containing metallacycles, the electronic coupling between adjacent ligands was relatively weak, whereas for the triangular phenanthrene-containing structures, there was a clear interaction between the conjugated ligand and the metal complex center. The transient lifetimes increased with increasing conjugation in that case. The results show that differences in the dimensionality and structure of metallacycles result in different optical properties, which may be utilized in the design of nonlinear optical materials and potential new, longer-lived excited state materials for further electronic applications.

Introduction

There is a need for superior organic and inorganic materials for advanced optical applications.[1] Organic chromophores and macromolecules have been investigated for their potential use in optical and electronic applications, and great progress has been made in substantially increasing the merit of these useful materials.[2] In addition to the various organic materials that have been probed for their optical effects, there has been interest in studying organometallic systems as well.[3−7] Many of these charge transfer materials have shown optical properties that are useful for optical limiting and other nonlinear optical effects.[8−11] The interaction of π structures with d-orbital metal centers has been utilized in electronic interactions that are important for novel applications.[12,13] Both metal-to-ligand (ML) and ligand-to-metal (LM) interactions have been exploited for intense absorption properties in the visible and near-IR spectral regions.[3−5]

Platinum-containing organometallic complexes have been extensively investigated for their applications in optical limiting.[14,15] These systems display singlet and triplet excitons in the visible and near-IR regions. In this regard, several platinum acetylene complexes have been synthesized and investigated in the literature to understand their applicability

[†] Department of Chemistry, University of Michigan.
[‡] Department of Macromolecular Science and Engineering, University of Michigan.
[§] Western Michigan University.
[||] East China Normal University.
[⊥] University of Utah.

(1) (a) Patil, A. O.; Heeger, J.; Wudl, F. *Chem. Rev.* **1988**, *88*, 183. (b) Tour, J. M. *Acc. Chem. Res.* **2000**, *33*, 791. (c) Zang, L.; Che, Y.; Moore, J. S. *Acc. Chem. Res.* **2008**, *41*, 1596. (d) Bredas, J. L.; Norton, J. E.; Cornil, J.; Coropceanu, V. *Acc. Chem. Res.* **2009**, *42*, 1699.
(2) Kohler, A.; Wilson, J. S. *Org. Elect.* **2003**, *4*, 179.
(3) Rogers, J. E.; Hall, B. C.; Hufnagle, D. C.; Slagle, J. E.; Ault, A. P.; McLean, D. G.; Fleitz, P. A.; Cooper, T. M. *J. Chem. Phys.* **2005**, *122*, 214708.
(4) Cooper, T. M.; Krein, D. M.; Burke, A. R.; McLean, D. G.; Rogers, J. E.; Slagle, J. E.; Fleitz, P. A. *J. Phys. Chem. A.* **2006**, *110*, 4369.
(5) Cooper, T. M.; Krein, D. M.; Burke, A. R.; McLean, D. G.; Rogers, J. E.; Slagle, J. E. *J. Phys. Chem. A.* **2006**, *110*, 13370.
(6) Silverman, E. E.; Cardolaccia, T.; Zhao, X.; Kim, K.-Y.; Haskins-Glusac, K.; Schanze, K. S. *Coord. Chem. Rev.* **2005**, *249*, 1491.
(7) Wong, W.-Y.; Ho, C.-L. *Coord. Chem. Rev.* **2006**, *250*, 2627.
(8) Tessler, N.; Denton, G. J.; Friend, R. H. *Nature* **1996**, *382*, 695.
(9) Rogers, J. E.; Slagle, J. E.; Krein, D. M.; Burke, A. R.; Hall, B. C.; Fratini, A.; McLean, D. G.; Fleitz, P. A.; Cooper, T. M.; Drobizhev, M.; Makarov, N. S.; Rebane, A.; Kim, K.-Y.; Farley, R.; Schanze, K. S. *Inorg. Chem.* **2007**, *46*, 6483.
(10) Slagle, J. E.; Cooper, T. M.; Krein, D. M.; Rogers, J. E.; McLean, D. G.; Urbas, A. M. *Chem. Phys. Lett.* **2007**, *447*, 65.
(11) Bhaskar, A.; Guda, R.; Haley, M.; Goodson, T. I. *J. Am. Chem. Soc.* **2006**, *128*, 13972.
(12) Varnavski, O. P.; Ranasinghe, M.; Yan, X.; Bauer, C. A.; Chung, S.-J.; Perry, J. W.; Marder, S. R.; Goodson, T., III *J. Am. Chem. Soc.* **2006**, *128*, 10988.
(13) Liu, Y.; Jiang, S.; Glusac, K. D.; Powell, D. H.; Anderson, D. F.; Schanze, K. S. *J. Am. Chem. Soc.* **2002**, *124*, 12412.
(14) Vestberg, R.; Westlund, R.; Eriksson, A.; Lopes, C.; Carlsson, M.; Eliasson, B.; Glimsdal, E.; Lindgren, M.; Malmström, E. *Macromolecules* **2006**, *39*, 2238.
(15) Guo, F.; Sun, W.; Liu, Y.; Schanze, K. *Inorg. Chem.* **2005**, *44*, 4055.

 10.1021/ja9082655

as nonlinear optical materials. They are also good systems for investigating excited-state phenomena such as excited-state absorption (ESA), intersystem crossing (ISC), triplet state absorption (TTA), two photon absorption,[11,16] excimers,[5] and phosphorescence.[4] Previous measurements have tailored the conjugated linkages that separate metal centers to promote the degree of $\pi-$d interactions, which are important for greater charge correlation throughout the structure. Many of the previous structures studied have been essentially linear with the metal in the center or at either end of the linkage. Several investigations demonstrated a strong charge correlation within the $\pi-$d interaction, which altered (in some cases enhanced) the electronic and nonlinear optical properties of the system. This gave strong justification for the creation of novel materials based on this organometallic motif for the enhancement of electronic interactions for specific optical applications.

While there have been a number of previous investigations that primarily focused on linear structures, the effects of the geometry of the organometallic system have received limited investigation. There is great cause to suggest that geometry plays an important role in the electronic transitions of different organometallic systems. Organic macromolecular systems with geometries varying from branched, cyclic, and flat two-dimensional motifs have been investigated by both steady-state and time-resolved measurements.[16−18] It has been found that the symmetry and degree of planarity in these systems is a critical factor in describing their optical excitations. In a similar manner, novel organometallic structures of varying geometry and/or symmetry may show similar correlations between structure and function.[19] Furthermore, only a few organometallic cage structures have had their fluorescent properties studied.[20] Advances in the synthesis of self-assembled Pt-containing metallacyclic and metallacage supramolecules of varying geometry (rectangular and triangular) and dimensionality (2D and 3D) allow for the steady-state and time-resolved properties of such supramolecules to be investigated.[21−27] Femtosecond measurements of fluorescence upconversion and transient absorption spectra have been studied for both the rectangular and triangular Pt-containing organometallic supramolecules in this contribution. The fluorescence lifetimes, as well as the transient absorption lifetimes, of the two architectures are compared. The effect of the charge transfer character is compared for a series of four different supramolecular rectangles, a series of three different supramolecular triangles, as well as a supramolecular cage structure. A model is proposed that describes the importance of particular excited-state mechanisms, which are dependent upon the macromolecular geometry. These findings suggest that the organometallic structures studied are good candidates for nonlinear optical materials and their optical properties can be tailored based on their geometry.

Experimental Section

a. Materials. Pt-anthracene acceptor **1**,[24] supramolecular rectangles **2**−**4**,[24] supramolecular triangles **5**−**7**,[25] and supramolecular metallacage **8**[26] were synthesized according to literature procedures (Figure 1). Further extentions to the rectangular clip design incorporating ethynyl functionality have recently been developed, although they were not studied in this manuscript.[27] The transient absorption and upconversion measurements were carried out in acetone (Aldrich) unless stated otherwise.

b. Steady-State Measurements. An Agilent UV−vis absorption spectrometer was used to obtain optical absorption spectra. A Jobin Yvon Spex Fluoromax-2 spectro fluorometer was used to determine the fluorescence spectra.

c. Two Photon Absorption Measurements. The two-photon excited fluorescence (TPEF) method involves monitoring the fluorescence intensity as a function of incident intensity. The laser source used in our experiments is either a Ti:Sapphire oscillator (Kapteyn Murnane) that can be tuned from 760 to 830 nm or an amplified system (Spectra-Spitfire) with an Optical Parametric Amplifier that can be tuned from 300 nm to 2 μm. The input intensity can be regulated using a neutral density (ND) filter designed for femtosecond pulses. The fluorescence is measured by a photomultiplier tube (PMT) (R7518P, Hamamatsu). A counting circuit (M8485 counting board, C3866 counting circuit, Hamamatsu) assembly, which is interfaced with a computer, converts the photocurrent from the PMT into an arbitrary number of counts. In this manner, the TPEF intensity can be quantified. A two-photon excited process is ensured when a logarithmic plot of the TPEF intensity versus input intensity is a straight line with a slope of 2.

d. Femtosecond Transient Absorption Measurements. Femtosecond transient absorption investigations have been carried out using ultrafast pump−probe spectrometer detecting in the visible region. This system contains 1-mJ, 100-fs pulses at 800 nm with a repetition rate of 1 kHz that were obtained from a Nd:YLF(Evolution)-pumped Ti:Sapphire regenerative amplifier (Spectra physics spitfire) with the input from a Millennia-pumped Ti:Sapphire oscillator (Spectra physics, Tsunami). The output of laser beam was split to generate pump and probe beam pulses with a beam splitter (85 and 15%). The pump beam was produced by an optical parametric amplifier (OPA-800). The pump beam used in the present investigation, that is, 420 nm, was obtained from the fourth harmonic of the idler beam and was focused onto the sample cuvette. The probe beam was delayed with a computer controlled motion controller and then focused into a 2-mm sapphire plate to generate a white light continuum. The white light is then overlapped with the pump beam in a 2-mm quartz cuvette containing the sample, and the change in absorbance for the signal is collected by a charge-coupled device detector (Ocean optics). Data acquisition is controlled by the software from Ultrafast Systems Inc. The typical energy probe beam is <0.1 μJ, while the pump beam is around $\sim$1−2 μJ per pulse. Magic angle polarization has been maintained between the pump and probe using a wave plate. Pulse duration has been obtained from the nonresonant fitting of the solvent response, which is around 120 fs. The sample is stirred by a rotating magnetic stirrer, and little degradation of the sample was observed during the experiments.

e. Fluorescence Upconversion Measurements. The fluorescence upconversion system used in our time-resolved experiments has been described previously.[29] To excite our samples, a FOG-

(16) Bhaskar, A.; Ramakrishna, G.; Hagedorn, K.; Varnavski, O. P.; Mena-Osteritz, E.; Bäuerle, P.; Goodson, T., III *J. Phys. Chem. B.* **2007**, *111*, 946.
(17) Goodson, T., III *Acc. Chem. Res.* **2005**, *38*, 99–107.
(18) Ramakrishna, G.; Bhaskar, A.; Goodson, T., III *J. Phys. Chem. B* **2006**, *110*, 20872.
(19) Yam, V. W. W. *Acc. Chem. Res.* **2002**, *35*, 555.
(20) Ghosh, S.; Mukherjee, P. S. *Organometallics* **2008**, *27*, 316.
(21) Stang, P. J.; Olenyuk, B. *Acc. Chem. Res.* **1997**, *30*, 502.
(22) Leininger, S.; Olenyuk, B.; Stang, P. J. *Chem. Rev.* **2000**, *100*, 853.
(23) Seidel, S. R.; Stang, P. J. *Acc. Chem. Res.* **2002**, *35*, 972.
(24) Kuehl, C. J.; Huang, S. D.; Stang, P. J. *J. Am. Chem. Soc.* **2001**, *123*, 9634.
(25) Kryschenko, Y. K.; Seidel, S. R.; Arif, A. M.; Stang, P. J. *J. Am. Chem. Soc.* **2003**, *125*, 5193.
(26) Kuehl, C. J.; Kryschenko, Y. K.; Radhakrishnan, U.; Seidel, S. R.; Huang, S. D.; Stang, P. J. *Proc. Natl. Acad. Sci. U.S.A.* **2002**, *99*, 4932.
(27) Ghosh, S.; Chakrabarty, R.; Mukherjee, P. S. *Inorg. Chem.* **2009**, *48*, 549.
(28) Bhaskar, A.; Ramakrishna, G.; Lu, Z.; Twieg, R.; Hales, J. M.; Haga, D. J.; Van Stryland, E.; Goodson, T., III *J. Am. Chem. Soc.* **2006**, *128*, 11840.
(29) Varnavski, O.; Goodson, T. *Chem. Phys. Lett.* **2000**, *320*, 688.

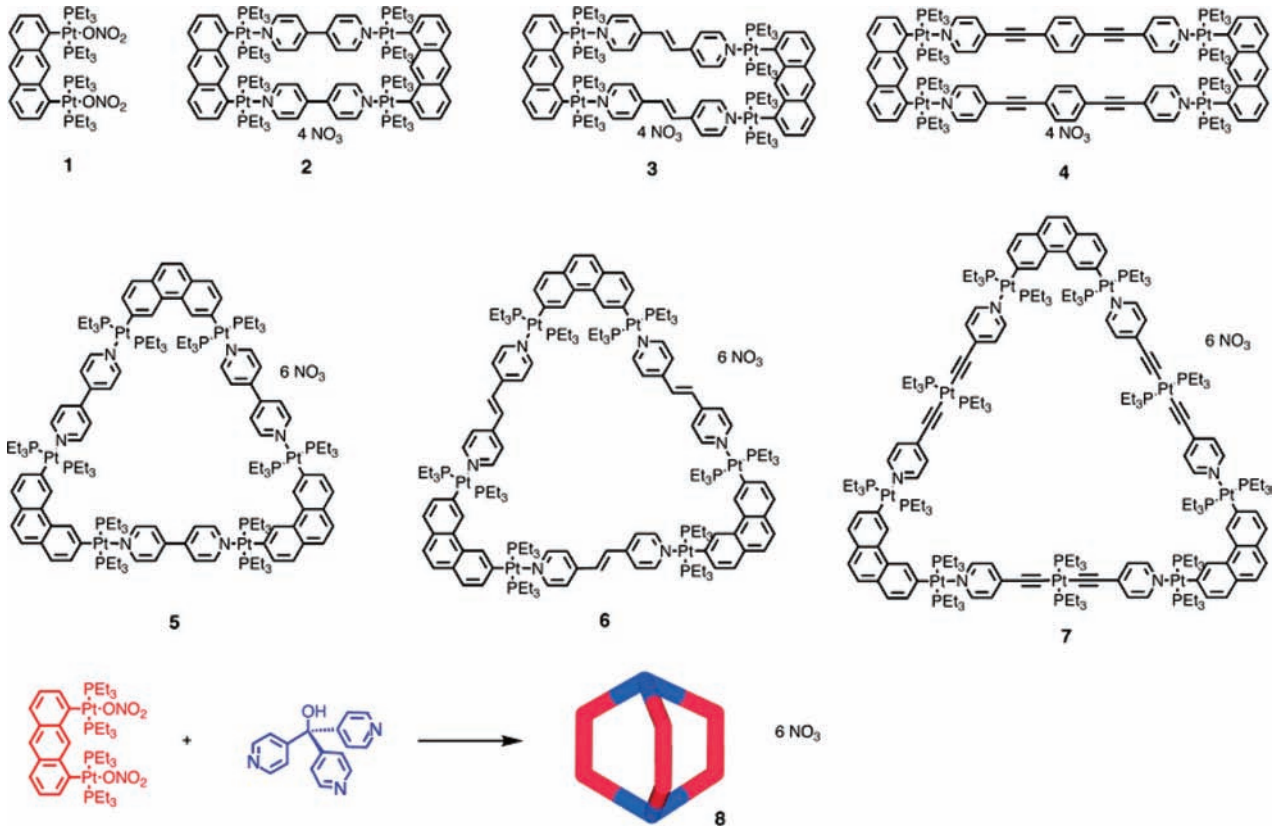

Figure 1. Molecular structures of the investigated organometallic monomer "clip" (**1**), metallacycles (**2**−**7**) and metallocage (**8**).

100 system (CDP) generates second harmonic light (400 nm) from a mode-locked Ti-sapphire laser. Polarization of the excitation beam for anisotropy measurements was controlled with a Berek compensator. All samples were held in a 1 mm thick rotating sample cuvette. Horizontally polarized fluorescence emitted from the sample was up-converted in a nonlinear crystal of β-barium borate using a pump beam at 800 nm, which first passed through a variable delay line. The instrument response function (IRF) was determined from the Raman signal of water. Lifetimes were obtained by convoluting the decay profile with the instrument response function. Spectral resolution was achieved by using a monochromator and photomultiplier tube. Under the experimental conditions, the organometallic complexes investigated were stable and no photodegradation was observed. To prove that the resulting ultrafast fluorescence is not a solvent artifact, measurements of acetone were carried out.

Results

A. Steady-State Absorption and Emission. Figure 2 shows the optical absorption data for organometallic compounds **1**−**4**. All the absorption spectra of these compounds show a vibronic progression that starts at 360 nm with the highest peak in the progression at 389 nm. Indeed, there is a strong similarity in absorption spectra of the first four (**1**−**4**) organometallic systems. The results suggest that the absorption consists of mainly $\pi-\pi^*$ transitions of anthracene whose conjugation might be extended into the Pt complex. The fact that there is only a small shift in the absorption spectra as the interior conjugation is increased suggests that the main transition is localized on the anthracene−Pt complex portion of the molecule. As the interior conjugation is increased from compounds **1** to **3**, the tail end of the absorbance spectrum increases. Upon further conjugation (**4**), the tail end of the absorbance spectrum is the same as that of compound (**3**). An increase in the tail end of the absorption, which spans into the visible region until 550 nm, suggests the presence of

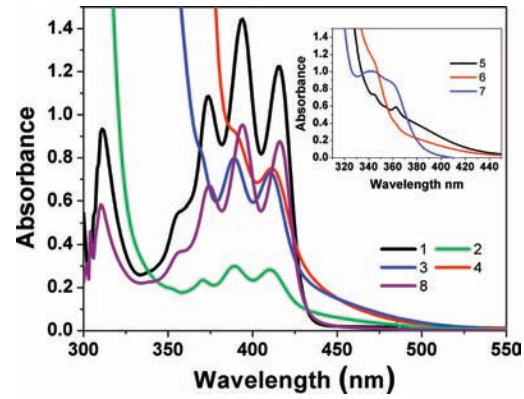

Figure 2. Steady-state absorbance spectra of compounds **1**−**4** and **8**. (Inset) Absorption spectra of compounds **5**−**7**.

intramolecular charge transfer effects or a metal−ligand charge transfer transition. It is possible to have the intramolecular charge transfer transitions from the anthracene−Pt complex to various acceptors in the rectangles 4,4′-bipyridine (**2**), *trans*-1,2-bis(4-pyridyl)ethylene (**3**), and 4-bis(4′-pyridylethynyl)benzene (**4**). Also shown in Figure 2 are the absorption spectra for the triangular organometallic complexes **5**−**7**. The presence of the strong vibronic procession that was found in the rectangles is absent for the metallacyclic triangles. This is primarily due to the weaker vibronic progression found in the phenanthrene complex, which is the main chromophore in the triangular organometallic supramolecules.[35] Instead, a long gradual transition is found with a maximum near 345 nm. Triangle **5** has two small noticeable absorption bands at 345 and 362 nm. Triangle **6** has a slightly red-shifted absorption spectrum with a noticeable shoulder at approximately 344 nm. Triangle **7** has

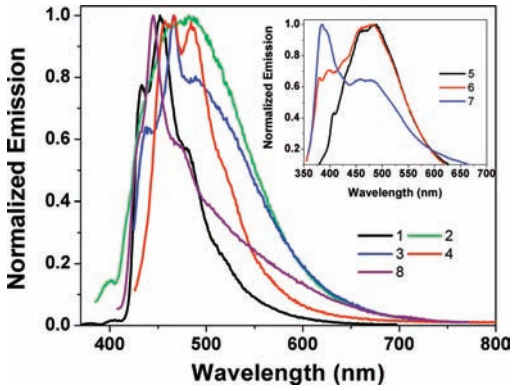

Figure 3. Normalized steady-state emission spectra profile for compounds **1**−**4** and **8**. (Inset) Emission spectra of **5**−**7**.

a broad peak at approximately 343 nm and a possible absorption band at 356 nm. The absorption in the visible region for these compounds, however, is mainly dominated by the charge transfer transitions arising out of metal−ligand or intramolecular charge transfer in these supramolecular metallacycles. Contrary to that of the supramolecular rectangles, the triangular systems show that the tail end of the absorption spectra amplitude decreases with increasing conjugation. It should be noted that in both series of supramolecular metallacycles, rectangular and triangular, there is very strong absorption deep in the UV. However, our time-resolved and nonlinear experiments are more concerned with the metal−ligand interactions found in the visible portion of the spectrum. Supramolecular metallacage **8** (Figure 2) was also studied. The vibronic progression observed in the rectangular series of supramolecules returns with a maximum near that which was found for anthracene-Pt(II) **1**. This observation is similar to previous studies of annulene systems and silsesquioxane.[30] In these systems, the principle $\pi \rightarrow \pi^*$ transition changed dramatically once the triangle or square was closed. The strongly coupled peaks observed in the absorption changed once the macrocycle was broken. It may be that in the present system, the Pt-ligand transfer is so dominant that intramolecular couplings are not strongly affected. In order to probe this process further we carried out time-resolved and nonlinear optical experiments.

Shown in Figure 3 are the optical emission data obtained for compounds **1**−**4**. For acceptor **1**, after excitation at 356 nm the emission has a strong peak at 472 nm, a smaller peak at 432 nm and a shoulder around 478 nm. For **2**, at 400 nm the emission maximum is shown to be much smaller than the larger peak at 475 nm. Rectangle **3** gives an emission spectrum peak at 435 nm and a larger peak at 466 nm. On the other hand, **4** has emission spectrum with two equivalent peaks at 458 and 485 nm. There is a strong similarity among organometallic systems **1**−**4**; all emission spectra have a maximum peak at approximately 470 nm. It is clear that by looking at the steady-state emission alone the anthracene−Pt complex appears to be the prevailing emitter. Also shown in Figure 3 are the emission spectra for the triangular organometallic complexes (**5**−**7**) as well as that of the metallacage (**8**). It is clear that increased interior conjugation results in an increasingly strong emission band at approximately 375 nm. The results of the emission spectra of triangles show that the emission in smaller triangles (**5**−**6**) is dominated by the intramolecular charge transfer while that of the largest triangle (**7**) has a measurable contribution from the phenanthrene, which has an emission maximum around 370 nm (Table 1).

Table 1. Steady-State Absorbance Peaks and Emission Peaks for All Compounds

material	λ_{abs}^{max} (nm)	λ_{em}^{max} (nm)
1	394	472
2	389	475
3	389	466
4	412	458, 485
5	∼400	485
6	∼400	474
7	343	382
8	394	446

In general, the steady-state absorption and emission results suggest that the optical excitations consist not only of individual chromophore $\pi-\pi^*$ transitions in the metallacycle but also of intramolecular or metal−ligand charge transfer transitions. Time-resolved and nonlinear optical property measurements were performed to give a better picture of the transitions and dynamics these systems.

B. Two- Photon Fluorescence. As stated in the introduction there has been great interest in the use of conjugated organometallic materials as optical limiters and in other nonlinear optical applications. Hence, we are interested in the femtosecond two-photon absorption response in the 700−900 nm spectral region. It was found that the length of conjugation in the ligands can have a strong effect on this process. Here, two photon fluorescence measurements were carried out to estimate the nonlinear cross sections in the Pt-containing organometallic structures. The two-photon fluorescence dependence was carried out using femtosecond (fs) pulses. Figure 4 shows the two photon fluorescence dependence for compounds **1** and **2**. The appropriate intensity dependence was found for these and other investigated metallacycle systems and a slope of 2, suggesting a two photon process, was observed. With fs pulses one is able to detect and measure the two-photon emission spectra of these and related systems (see Figure 4). For these macrocycles the spectrum extends over a relatively broad range. These photonic properties could indeed be useful for applications in sensors and optical limiting devices. While the amount of two photon fluorescence was large, due to the relatively small quantum yield ($\sim 10^{-4}$) for linear fluorescence in the sample, the calculated two photon cross-section was small (∼10 GM). These results suggest that the time-scale of the two-photon measurement may be very fast and the contribution from the triplet state could be small. Previous results with other linear platinum-containing systems showed an increase in the cross-section with increasing delocalization over the ligands.[31] Here, it appears that the two-photon excitation may be localized on each ligand and the main contribution comes from a metal-to-ligand excitation. This, however, cannot be concluded from steady-state and two-photon measurements alone.

C. Fluorescence Upconversion Measurements. Time-resolved measurements of the excited state and relaxed states are necessary to more accurately probe the dominate structural/electronic factors in these systems. In the case of relaxed states, fluorescence upconversion experiments were used to probe fluorescence lifetimes over a wide degree of time scales for the purpose of detecting long-range interactions. Here, we are

(30) Sulaiman, S.; Bhaskar, A.; Zhang, J.; Guda, R.; Goodson, T., III; Laine, R. M. *Chem. Mater.* **2008**, *20*, 5563.

(31) Ramakrishna, G.; Goodson, T., III; Rogers-Haley, J. E.; Cooper, T. M.; McLean, D. M.; Urbas, A. J. *Phys. Chem. C* **2009**, *113*, 1060.

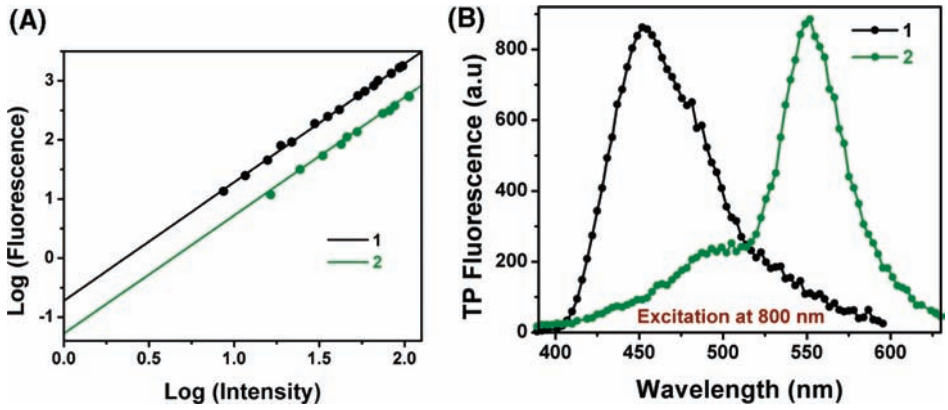

Figure 4. (A) Two photon measurement intensity dependence. (B) Two photon fluorescence spectrum.

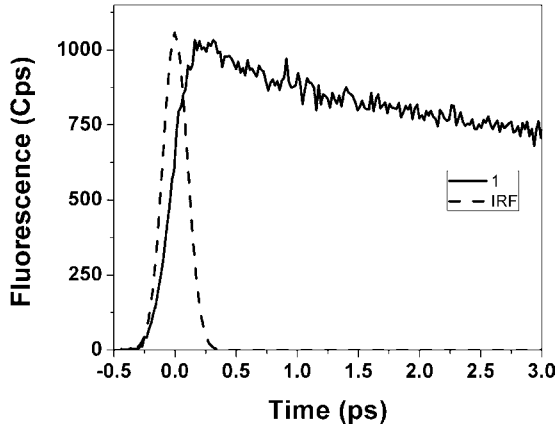

Figure 5. Time-resolved fluorescence upconversion of **1** at 480 nm with an excitation at 400 nm. Instrument response function is also shown.

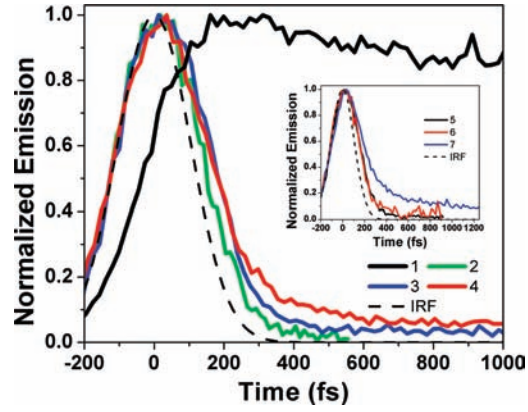

Figure 6. Time-resolved fluorescence decay of compounds **1**−**4** excited at 400 nm. **1** is in black, **2** is in red, **3** is in green, **4** is in blue, and the instrument response function is the black dashed line. (Inset) Fluorescence decay of compounds **5**−**7**.

interested in the variation of the fluorescence lifetimes as a function of the chain linkage in the metal centered metallacycles as well as variations due to changes in geometry. Shown in Figure 5 is a representative fluorescence upconversion decay curve for the bis-Pt(II) anthracene **1** at 480 nm. The fluorescence decay profile is best fit by a single exponential given as: $f(x) = Ae^{(-t/\tau)}$. The lifetime for this particular system excited at 400 nm is 8.9 ± 0.2 ps, which can be ascribed to either the intramolecular charge transfer rate or the intersystem crossing to triplet state. This lifetime differs from what has been observed in linear organometallic systems, which in the past have shown fluorescence decay times of 70 ± 40 fs.[31] This discrepancy is due not only to the nonlinear geometry but also to the metal interaction with the anthracene molecule. The lifetime is shorter than the typical fluorescence lifetime of anthracene (3.9 to 6.2 ns).[32] This suggests that the excitation is delocalized up to the metal atom where a fast ISC process dominates its excited state deactivation.

Figure 6 shows the time-resolved fluorescence decay at 480 nm for metallacyclic structures **1**−**4** after excitation at 400 nm. The insert of Figure 6 gives the time-resolved fluorescence decay for samples **5**−**7**. The fluorescence decay of **1** is long-lived with respect to the remaining organometallic complexes discussed in this article. The fluorescence decay of complexes **2**−**4** are extremely fast and therefore close to the instrument response function with a pulse width of 110 fs. The average lifetimes of **2** and **3** at 480 nm were found (after deconvolution) to be 110 ± 50 fs and 140 ± 60 fs, respectively. The average lifetime of **4** was found to be 160 ± 60 fs also indicating the presence of a long-lived second component. The fluoresce decay of the triangular samples **5**−**7** showed similar dynamics with increasing size. Triangle **5** has a lifetime of 130 ± 50 fs, while **6** has a lifetime of 110 ± 40 fs. The fluorescence decay of **7** varried from those of **5** and **6**, having a decay fit with a biexponential with a large 190 ± 60 fs component and a small remaining component with a lifetime of 2.4 ± 0.1 ps. Upconversion fluorescence decay lifetimes are listed in Table 2.

Table 2. Average Lifetimes of All Upconversion Fluorescence Sample Decays Monitored at 480 nm

material	average lifetime
1	8.9 ± 0.2 ps
2	110 ± 50 fs
3	140 ± 60 fs
4	160 ± 60 fs
5	130 ± 50 fs
6	110 ± 40 fs
7	190 ± 60 fs
	2.4 ± 0.1 ps

Upconversion fluorescence decay has also been studied at emission wavelengths of 450 nm, 500 nm, 520 nm, 550 and 570 nm resulting in variations in the kinetic time constants. Metallacycles **4** and **7** are representative of the upconversion fluorescence decay lifetimes' emission wavelength dependence and are presented in Figure 7 (with sample **7** in the inset). The remaining supramolecular rectangular and triangular fluores-

(32) Birks, J. B. *Photophysics of Aromatic Molecules*; Wiley: London, 1970.

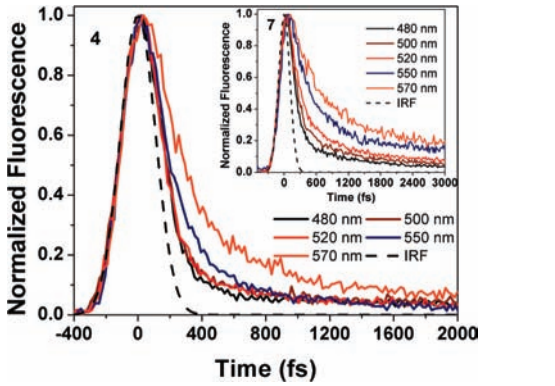

Figure 7. Time-resolved fluorescence decay for compound **4** at different wavelengths. (Inset) Time-resolved fluorescence decay for triangle **7**.

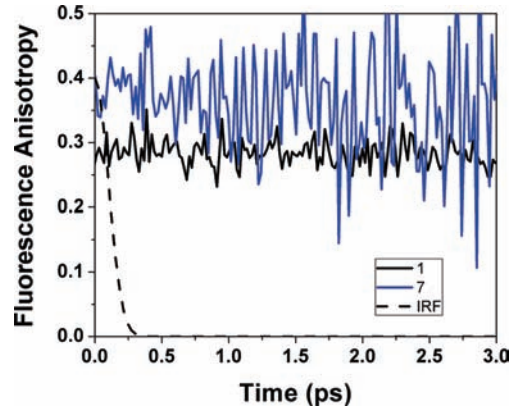

Figure 8. Fluorescence anisotropy of **1** and **7** with instrument response function.

cence plots are shown in the Supporting Information. Femtosecond fluorescence relaxation processes at different emission wavelengths have been investigated previously. For example, in our previous studies we have shown that the fluorescence dynamics of dendrimers at different emission wavelengths can be very important.[33] In this study, the biexponential lifetime dependence on emission wavelength was in accordance with the formation of two fluorescence states. Such processes are also associated with the formation of aggregates such as excimers or exciplexes. In the discussion of this wavelength dependence on the fluorescence lifetime, an intermediate trap state best explains the process. Justification for this conclusion comes from the short formation lifetime as compared to the relaxation rates. In the metallacycles studied, it was found that with increasing emission wavelength there was an increase in the average fluorescence lifetime. The lifetimes are described by a biexponential decay, with one lifetime being between 100−500 fs and the other lifetime being between 1−6 ps. What is not observed, however, is the long rise time feature found in the dendrimer systems referenced above. This suggests that while there is a strong justification for increased charge-transfer behavior in these systems there may not be a localized intermediate trap state.

D. Anisotropy Measurements of Energy Migration. The fluorescence upconversion investigations give information about excited state lifetimes as well as the energy migration throughout each system. This can be accomplished through fluorescence anisotropy measurements. The depolarization of the fluorescence as a function of time can be evaluated with very good time resolution by time-resolved fluorescence upconversion. Previous investigations with femtosecond anisotropy measurements have shown the importance of intramolecular interactions to the enhancement of transition moments and nonlinear optical effects.[31] The differences in energy migration and reorientational dynamics in particular systems may point to specific structure−function relationships critical to the design of superior materials. Shown in Figure 8 is a representative fluorescence anisotropy decay result for compounds **1** and **7** out to 3 ps. The noise experienced is due to the weaker signal at long times with the fast anisotropy dynamics essentially completed by this time. The measured initial anisotropy for the case of **1** was near 0.28. Over the 8 ps time scale there was little to no detectable decay of the anisotropy. The remaining rectangular samples had slightly higher anisotropy values with compound **2** having 0.36, **3** having 0.33 and **4** having 0.3. The triangular metallacycles had anisotropies of 0.37 for **5**, 0.37 for **6** and 0.35 for **7**.

For the case of a simple transition moment oscillator system, the initial anisotropy value should be 0.4. The high initial anisotropy (slightly less than 0.4) for all the rectangular and triangular metallocycles confirms that the emission is coming from localized transition dipoles and the emission is not delocalized. The localized excitations are in accordance with the observed intramolecular charge transfer processes in the investigated organometallic systems. The coupling between nearby energy levels accessible to the transition may also give rise to the lower initial anisotropy value. Typically the anisotropy decays from 0.4 to 0. In our systems, there is no discernible anisotropy decay, suggesting that the angle between the emitting and absorbing transition dipoles remains unchanged during intersystem crossing, which is suggestively fast. In our previous measurements we have observed similar effects in square like symmetric chromophores, cyclic geometry systems, dendrimer systems and linear systems.[16,31,33] These results suggest that the electronic excitation may be localized on one of the chromophores and that the complex excited-state dynamics is entirely directed by intrachromophore processes.

E. Transient Absorption Measurements. While time-resolved fluorescence upconversion provides important details about relaxed states in the supramolecular rectangular and triangular systems, ultrafast transient absorption experiments give important details about the excited-state dynamics and amplitudes critical to triplet and singlet lifetimes as well as extent of charge transfer character. Measurements of the excited state lifetimes have been carried out with these systems to probe the changes in charge transfer character with different sized linkers.

Figure 9 shows the transient absorption spectrum of compounds **1**−**4**. Figure 10 (top left) shows the spectrum of **1**, in which a decay of the excited state absorption (ESA) at a wavelength of 620 nm concomitant growth of ESA at 490 nm is observed. ESA at 490 nm can be ascribed to the triplet−triplet state absorption of anthracene. The lifetime of the ESA is ∼20 ps and corresponds with the growth of ESA with a time constant of 22 ± 1.0 ps for the 490 nm kinetics. The kinetic analysis of the absorption at 620 nm showed a lifetime of 17.1 ± 0.44 ps. The isosbestic point at approximately 545 nm is typical of conversion between the triplet and relaxed triplet state. The spectrum of compound **2** (Figure 9) shows the decay of the ESA with a maximum around 650 nm from 100 fs to 1 ps, which arises from an intramolecular charge transfer from anthracene to bipyridyl. The fast component observed in the

(33) Varnavski, O.; Leanov, A.; Liu, L.; Takacs, J.; Goodson, T., III *Physical Review B.* **2000**, *61*, 12732.

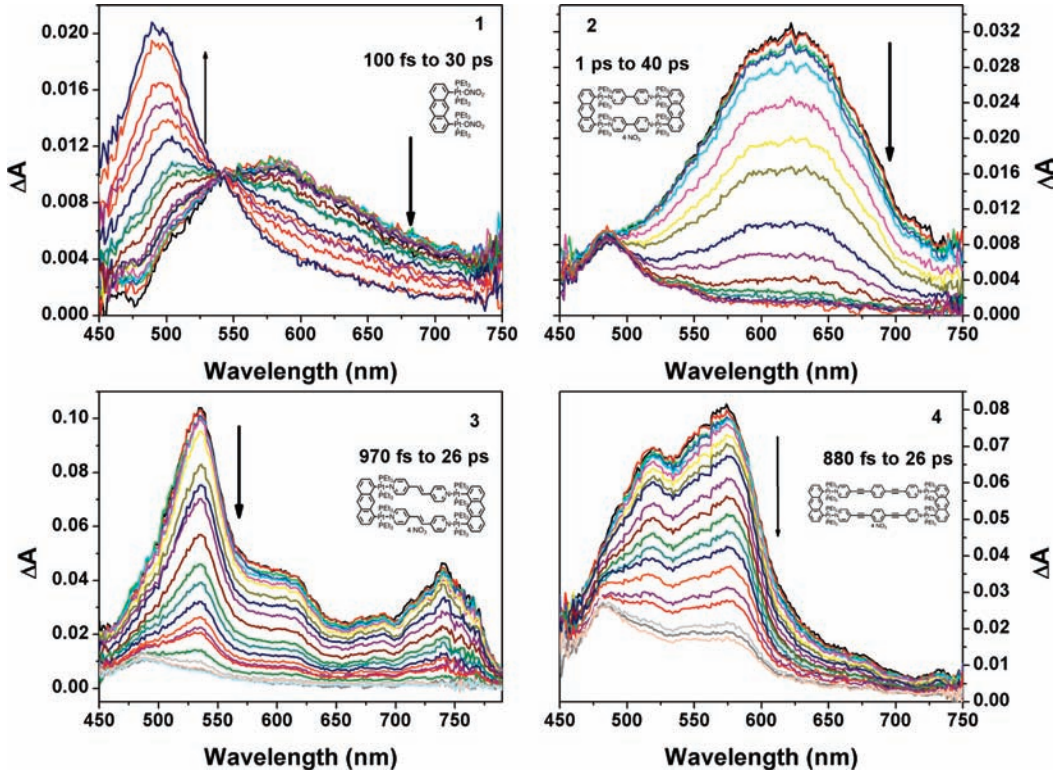

Figure 9. Transient absorption spectrum of compounds **1**−**4** in acetone at various time delays. (Top Left) Spectra of **1** after excitation at 390 nm, 100 fs to 30 ps. (Top Right) Spectra of **2** after excitation at 390 nm, 1 to 40 ps. (Bottom Left) Spectra of **3** after excitation at 390 nm, 30 to 750 ps. (Bottom Right) Spectra of **4** after excitation at 390 nm, 880 fs to 26 ps.

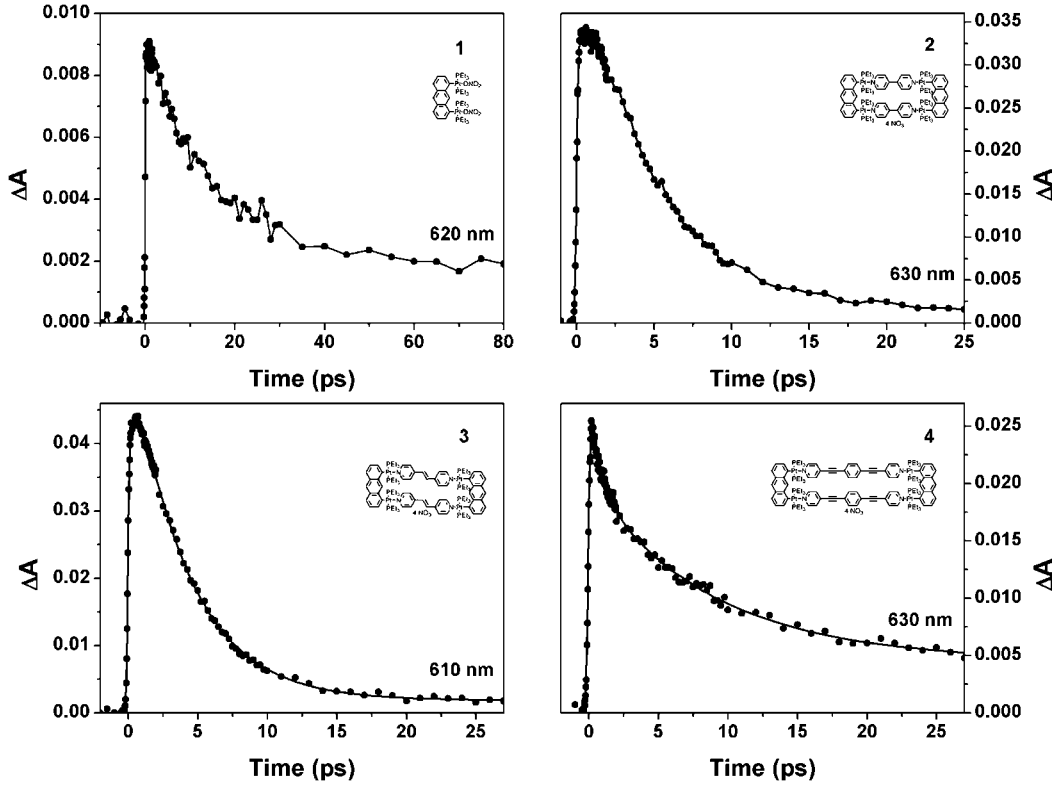

Figure 10. Kinetic decays for the transient absorption spectrum of compounds **1**−**4** in acetone at various time delays. (Top Left) Kinetics of **1** after excitation at 390 nm. (Top Right) Kinetics of **2** after excitation at 390 nm. (Bottom Left) Kinetics of **3** after excitation at 390 nm. (Bottom Right) Kinetics of **4** after excitation at 390 nm.

fluorescence matches with the intramolecular electron transfer rate. However, the broad ESA (Figure 9, top right) decayed very quickly to give rise to absorption around 480 nm, reminiscent of triplet−triplet ESA of the anthracene-Pt complex.

Table 3. Transient Absorption Average Lifetimes for Samples **1**−**4**

	transient absorption kinetics	
material	wavelength (nm)	time (ps)
1	620	17.1 ± 0.44
2	630	6.05 ± 0.09
3	610	4.49 ± 0.07
4	630	6.47 ± 0.24

The results show that there is an ultrafast forward electron transfer followed by recombination with time scales of 6.05 ± 0.09 ps for **2**.

The results indicate that the recombination is producing the triplet state exciton, which is long-lived though not as efficient as the anthracene-Pt complex. Interestingly, a completely different transient spectrum is obtained for compounds **3**−**4**. The ultrafast growth of the intramolecular charge transfer and consequent recombination gives rise to a triplet state due to the anthracene-Pt complex is observed for sample **3**. This is evident from the entirely different transient absorption spectrum for **3**, as it has different transient radical species with the anion located on the bipyridyl stilbene that has a typical ESA spectrum.

The transient absorption growth and decay are also observed for organometallic rectangle **4**, with different transient spectra arising out of the ICT from anthracene-Pt complex to the anion radical present in the metallacycle **4**. The lifetimes of the charge separation and recombination are obtained from the global fit analysis of the kinetic decay trace (Figure 10). Also, the kinetic decay traces at two different wavelengths, representing the ESA of the ICT state and the triplet−triplet absorption are seen in Figure 10. The decay lifetime was 22.0 ± 1.0 ps for compound **1**. The substantial difference between bis-Pt(II) anthracenyl acceptor **1** and rectangular supramolecules **2**−**4** suggests stronger intramolecular interactions leading to different charge transfer character and lifetimes. Table 3 outlines the various transient absorption kinetics and the charge separation and recombination lifetimes.

Figure 11 shows the transient absorption spectrum of triangular metallacycles **5**−**7**. For **5**, it can be observed that there is a growth of the excited state absorption with a maximum near 600 nm and a growth at 450 nm. At 490 nm, the kinetic decay for compound **5** is described by a biexponential decay with lifetimes of 5.7 ± 0.4 fs and 114.8 ± 8.9 fs. At 640 nm, the kinetic decay gives the biexponential decay lifetimes of 10.5 ± 0.7 fs and 150 ± 5.4 fs. The extremely fast lifetime decay for compound **5** is drastically different from that of the other systems studied. This suggests extremely fast ICT. Compound **6** displays a similar transient absorption profile with a maximum near 525 nm. At 525 nm a single exponential lifetime decay of 8.1 ± 0.2 ps is observed, while at 565 nm an exponential lifetime decay of 6.7 ± 0.2 ps is found. These two lifetimes are evident of triplet state relaxation. Interestingly a completely different transient spectrum is obtained for metallacycle **7**. A maximum excited state absorption was found at 555 nm with an isosbestic point at 525 nm. Again, the isosbestic point suggests conversion between the triplet and relaxed triplet state. The lifetimes of the charge separation and recombination for the triangular supramolecules are obtained from the global fit analysis of the kinetic decay trace (Figure 12). The kinetic decay traces at two different wavelengths representing the ESA of ICT state and the triplet−triplet absorption are seen in Figure 12. The average exponential lifetime of **7** is 21.5 ± 0.7 ps at 460 nm. As observed for compounds **2**−**4**, the substantial difference for triangle **7** from the other supramolecular triangles may be attributed to stronger intramolecular interactions leading to

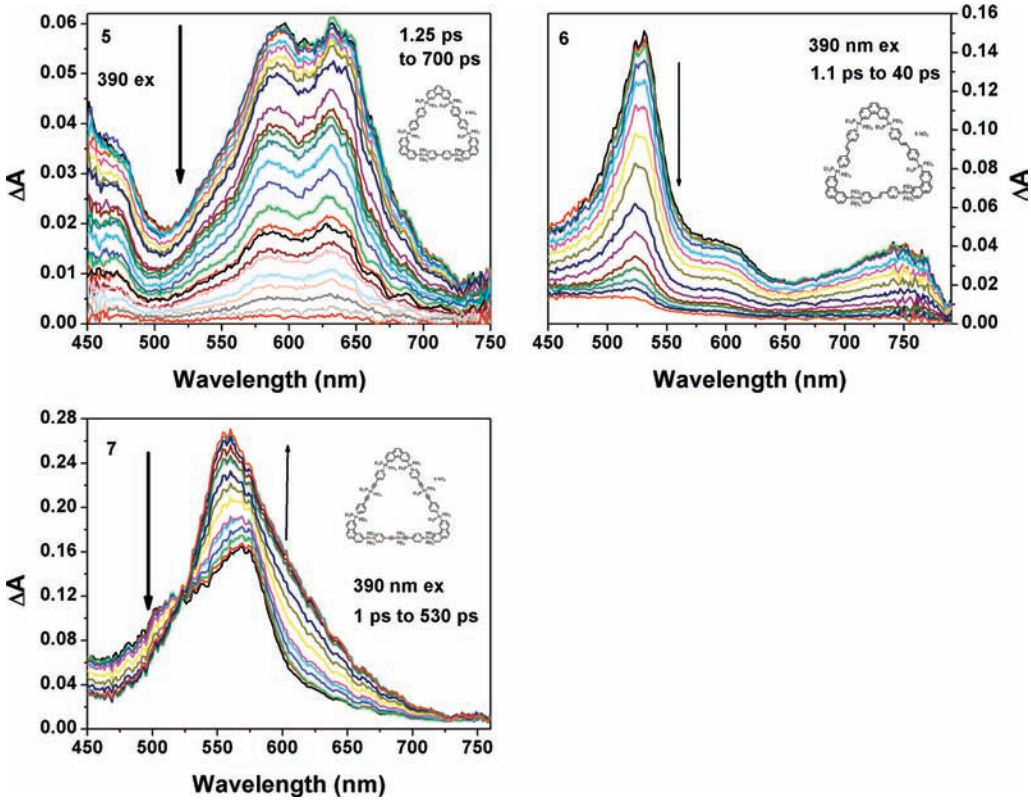

Figure 11. Transient absorption spectra of triangles **5**−**7** in acetone at various time delays. (Top Left) Spectra of **5** after excitation at 390 nm, 1.25 to 700 ps. (Top Right) Spectra of **6** after excitation at 390 nm, 1.1 to 40 ps. (Bottom Left) Spectra of **7** after excitation at 390 nm, 1 to 530 ps.

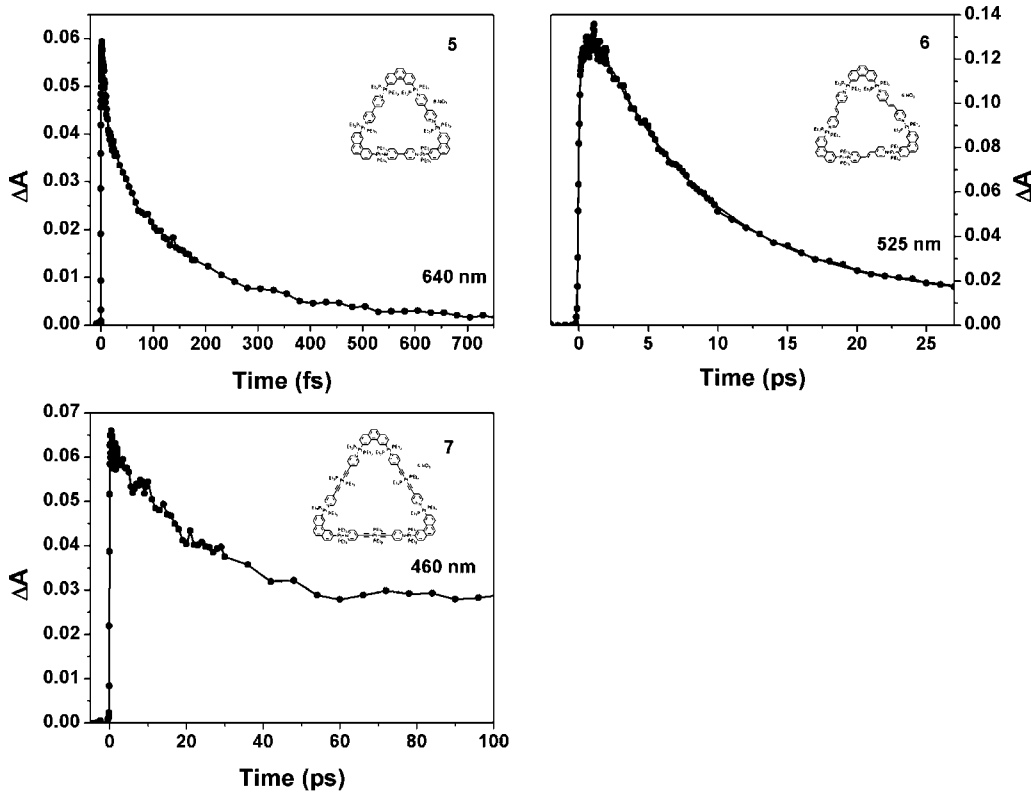

Figure 12. Transient absorption kinetics for supramolecular triangles **5**−**7**.

Table 4. Transient Absorption Average Lifetimes for Samples **5**−**7**

transient absorption kinetics		
material	wavelength (nm)	time (ps)
5	640	0.184 ± 0.006
6	525	8.1 ± 0.2
7	460	21.9 ± 0.9

different charge transfer characters and lifetimes. Table 4 gives their transient absorption kinetic lifetimes.

F. Three-Dimensional Metallacage. A three-dimensional metallacage (**8**) was studied to investigate the role that dimensionality plays in charge transfer dynamics. Toward this aim, steady-state measurements, fluorescent upconversion and transient absorption measurements were carried out. Figure 13 displays the upconversion lifetimes, transient absorption, transient kinetics and anisotropy measurements of metallacage (**8**). Compound **8** displays similar absorbance spectra to that of compound **1** with a high peak at 446 nm and a vibronic progression of 423 nm, 472 nm, and 500 nm as the main chromophore is similar to that of compound **1**. The shoulder at 423 nm is similar to that of the lower peak for compound **1**, while the shoulder at 472 nm of the metallacage lines up with the highest peak of **1**. The metallacage emission spectrum differs from compound **1** in that it has a much stronger tail into the red. This again accounts for the larger cage structure of compound **8**, which contains three bis-Pt(II) anthracenyl moieties (**1**). The fluorescence upconversion decay lifetimes are described by a biexponential decay for 450 nm, 480 nm, and 500 nm, and 520 nm. With increasing emission wavelength, increasing fluorescence lifetimes are found for both the short and long decay processes, indicating the presence of intramolecular charge transfer interactions. At 480 nm a short lifetime of 420 fs and a long lifetime of 2.4 ps were observed. At 520 nm, a short lifetime of 760 fs and a long lifetime of 4.3 ps were found.

Transient absorption experiments were carried out giving a maximum excited state absorption at approximately 482 nm with an inflection point at 542 nm and two smaller absorption peaks at 590 nm and 745 nm. The lifetimes of the charge separation and recombination for the metallacage were described by a biexponential decay with a lifetime of 1.1 and 32.2 ps at 600 nm. In general, while the cage compound shows a higher degree of complexity in structure, the dynamics appeared to be very similar to what was found with the metallacycles investigated.

Discussion

The goal of this investigation was to probe the differences in charge transfer character, triplet state relaxation, excited fluorescence dynamics and potential nonlinear optical and electronic applications. The observed results suggest that these metallacycles vary in their triplet state relaxation when the square like geometry is changed to the triangular system. The kinetic schemes for excitations in similar organometallic complexes have been illustrated in previous reports.[31] For informative reasons a variation of this diagram is reproduced in Figure 14. As seen in the diagram, a chromophore is excited from the ground state S_0 to the S_1 state. ISC allows for the S_1 state to transition to the T_1 state, which then decays to the ground state. Femtosecond fluorescence upconversion is used to determine the extent of ISC and singlet decay while transient absorption is determines the TTA and ESA. In our previous study regarding the platinum acetylene complexes, ISC time increased with ligand length.[31] It is understood that the increased π^* character as well as the decreased heavy atom effect were the factors for the increased ISC lifetime. In the current study, increasing ligand length was accomplished by substitution of the different ligands 4,4′-Bipyridine (**2**,**5**), *trans*-1,2-bis(4-

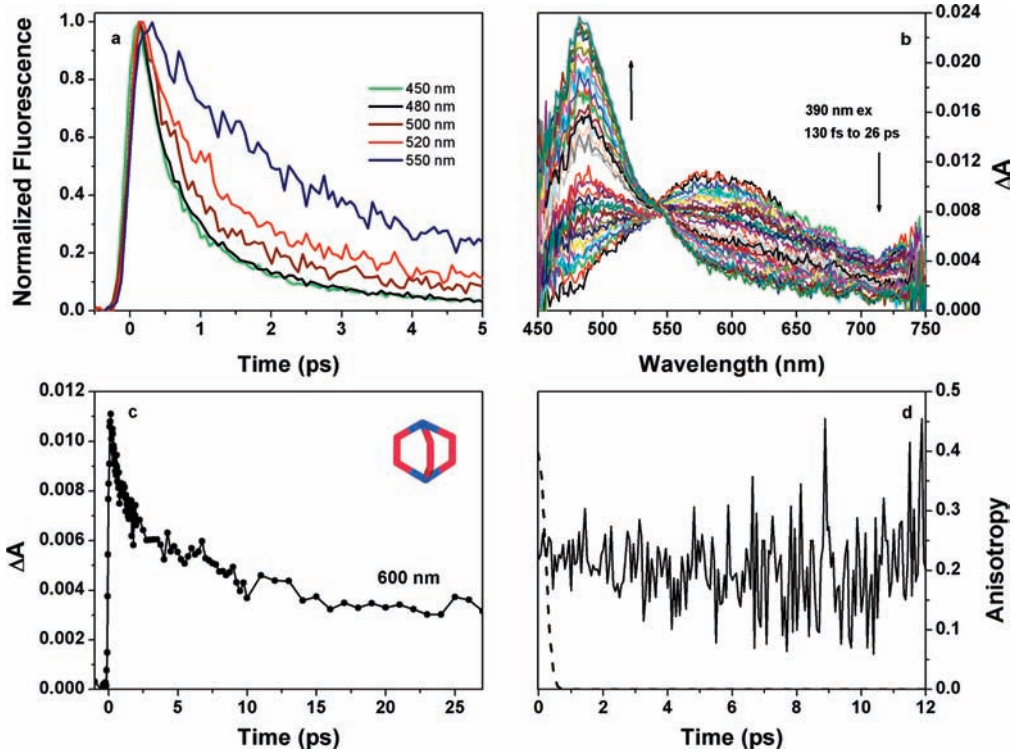

Figure 13. Metallacage (a) fluorescence upconversion lifetimes, (b) transient absorption spectrum, (c) transient absorption kinetics, and (d) anisotropy.

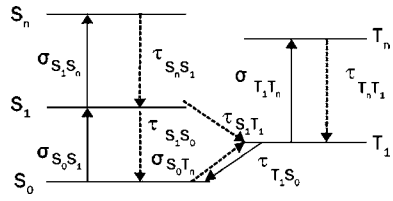

Figure 14. Kinetic scheme for the organometallic complexes.

pyridyl)ethylene (**3**,**6**) and 1,4-bis(4′-pyridylethynyl)benzene (**4**) and *trans*-[bis(4-pyridylethynyl)bis(triethylphosphine)]platinum-(II) (**7**). The compound with the longest fluorescence lifetime was the bis-Pt(II) anrthracenyl acceptor (**1**). Upon conjugation, the ISC time dramatically decreased. The dramatic decrease in ISC lifetime (in the 100 fs range) typically suggests very strong spin−orbit coupling due to the presence of the Pt metal. Since this was not the case for compound **1**, it is believed that conjugation was the determining factor for the ultrafast fluorescence (ISC) results. However, as shown earlier, the charge transfer contribution to the observed dynamics depends on the nature of the bridging ligand and its energetics rather than the conjugation length. For the rectangular organometallic structures, further conjugation showed evidence of slightly increasing ISC times although all lifetimes were within the experimental error. For the triangular organometallic compounds, organometallic triangle **6** displayed a slightly decreased lifetime with respect to triangle **5**, although again this was also within the error. Interestingly, compound **7** showed a dramatic increase in the lifetime from that of **5** and **6**. This result is unexpected given that the ligand contains more platinum atoms, which should result in a shorter ISC lifetime. A possible reason for this can be because of the presence of weaker charge transfer interactions which increases the fluorescence lifetime. It can be observed from the absorption measurements that the charge transfer absorption for **7** is significantly lower than **5** and **6**. A comparison of the rectangular and triangular organometallic structures shows considerable similarities. Both systems have ultrafast ISC, an increase in ISC with increasing conjugation, and emission wavelength dependence. However, the large ISC lifetime variation between compounds **4** and **7** was not expected. This can possibly be attributed to the anthacene moiety as well as to different ligands.

Metal-to-ligand charge transfer processes with varying degrees of conjugation in the ligands has been investigated in the past. For example, Ren et al. investigated such charge transfer processes in oligoynes.[34] It was found that for the case of linear absorption, the low energy metal-to-ligand charge transfer band has a significant shift to lower energy as the ligand-conjugation is increased. It was also found that as the π character is increased in the ligand the charge transfer character also changed for the complex, which follows from basic electron transfer molecular processes. The drastic difference in lifetimes for the triangular organometallic cages **5**−**7** gives evidence for the charge transfer character dependence on increased conjugation. Such variations in lifetimes with similar steady-state absorption profiles demonstrates that the steady-state profiles alone are not capable of describing the complexities of the charge transfer within organometallic systems.

Conclusion

Using femtosecond upconversion and transient absorption, we have measured and characterized the ultrafast excited state relaxation dynamics of platinum containing organometallic metallacycles. Typically a biexponential decay was capable of describing the two fluorescence species. We found

(34) Xu, G. L.; Wang, C. Y.; Ni, Y. H.; Goodson, T., III; Ren, T. *Organometallics* **2005**, *24*, 3247.
(35) Murov, S. L.; Carmichael, I.; Gordon, L. H. *Handbook of Photochemistry*; Marcel Dekker Inc: New York. 1973.

intramolecular charge transfer processes giving rise to charge-separated species followed by charge recombination to give rise to the triplet exciton. One species is the decay of immediate ESA ascribed to singlet state. The other observed species is a long-lived excited state, which is ascribed to triplet−triplet absorption of anthracene and phenanthrene. It was determined that the presence of platinum influences the spin−orbit coupling and increases the rate of ISC while decreasing the lifetime of the singlet state. The rectangular structures show similar transient lifetimes within the series studied. However, the triangular systems showed a strong and definite effect on the ligand conjugation. A consistent increase in the lifetime was observed as the conjugation of the ligand unit next to the metal center was increased. The triangular unit, for this reason, is a great candidate for nonlinear optical and optical limiting effects.

Acknowledgment. P.J.S. thanks the NIH (GM-57052) for support. B.H.N. thanks the NIH (Grant GM-080820) for support. T.G.III thanks AFOSR and NSF (polymers) for support.

JA9082655